GPS Solutions (2024) 28:93
https://doi.org/10.1007/s10291-024-01630-w

ORIGINAL ARTICLE

Ionospheric corrections tailored to Galileo HAS: validation with single-epoch navigation

C. C. Timote[1] · J. M. Juan[1] · J. Sanz[1] · A. Rovira-Garcia[1] · G. González-Casado[1] · R. Orús-Pérez[2] · I. Fernández-Hernández[3] · D. Blonski[2]

Received: 27 October 2023 / Accepted: 26 February 2024 / Published online: 26 March 2024
© The Author(s) 2024

Abstract

The Galileo high accuracy service (HAS) is a new capability of the European global navigation satellite system, currently providing satellite orbit and clock corrections and dispersive effects such as satellite instrumental biases for code and phase. In its full capability, Galileo HAS will also correct the ionospheric delay on a continental scale (initially over Europe). We analyze a real-time ionospheric correction system based on the fast precise point positioning (F-PPP), and its potential application to the Galileo HAS. The F-PPP ionospheric model is assessed through a 281-day campaign, confirming previously reported results, where the proof of concept was introduced. We introduce a novel real-time test that directly links the instantaneous position error with the error of the ionospheric corrections, a key point for a HAS. The test involved 15 GNSS receivers in Europe acting as user receivers at various latitudes, with distances to the nearest reference receivers ranging from tens to four hundred kilometers. In the position domain, the test results show that the 95th percentile of the instantaneous position error depends on the user-receiver distance, as expected, ranging in the horizontal and vertical components from 10 to 30 cm and from 20 to 50 cm, respectively. These figures not only meet Galileo HAS requirements but outperform them by achieving instantaneous positioning. Additionally, it is shown that formal errors of the ionospheric corrections, which are also transmitted, are typically at the decimeter level (1 sigma), protecting users against erroneous position by weighting its measurements in the navigation filter.

Keywords Ionospheric modeling · Precise navigation · PPP · Galileo HAS

Introduction

Zumberge et al. (1997) introduced the precise point positioning (PPP) technique, consisting of generating precise corrections for satellite orbits and clocks from which the user can achieve a position solution with error at the centimeter level in static positioning and about one decimeter in kinematic mode. Initially developed and applied in post-processing mode, PPP's main drawback was the convergence time required for achieving a precise navigation solution: from several tens of minutes, in multi-constellation, to hours in single constellation (Juan et al. 2012). Nowadays, PPP convergence time can be reduced thanks to multi-constellation, multi-frequency, and ambiguity resolution (AR) techniques, as shown by Duong et al. (2020), enabling the real-time computation of PPP precise corrections, as it is done in the real-time service (RTS) of the International GNSS Service (IGS), see, for instance, Hadas and Bosy (2015).

Recent studies have demonstrated that by employing such real-time corrections, within a multi-constellation framework and utilizing up to four frequencies, it is possible to almost obtain instantaneous precise navigation when all carrier phase ambiguities are fixed. This capability is highlighted in works such as Laurichesse and Banville (2018) and Naciri and Bisnath (2023). Nevertheless, in the case of a dual-frequency receiver, the fast convergence is reliant

✉ J. M. Juan
jose.miguel.juan@upc.edu

[1] Research Group of Astronomy and Geomatics (gAGE), Universitat Politècnica de Catalunya (UPC), José Miguel Juan, Jordi Girona, 1-3, 08034 Barcelona, Spain

[2] Wave Interaction and Propagation Section, European Space Agency (ESA), Noordwijk, The Netherlands

[3] Directorate-General for Defence Industry and Space (DEFIS), European Commission (EC), Brussels, Belgium

on external ionospheric corrections, as it is done using the real-time kinematic (RTK) technique.

In this sense, to obtain a precise navigation solution after some tens of seconds, RTK can also be used. The concept of PPP–RTK, as defined in Wübbena et al. (2005), complements precise corrections from a PPP service provider with ionospheric corrections obtained through a linear interpolation of ionospheric delays from a network of permanent receivers.

The challenge with PPP–RTK is that computing accurate ionospheric corrections and significantly reducing the convergence time requires baselines between permanent receivers to be no larger than one or two hundred kilometers. This reduced baseline distance would require hundreds of permanent receivers to provide continental-scale service coverage, as rover receivers are usually located some tens of kilometers from the reference stations (Psychas et al. 2018).

The Galileo high accuracy service (HAS) is a new capability of the European global navigation satellite system. After completing testing and experimentation during "Phase 0", Galileo HAS started the so-called "Phase 1", in which its initial Service Level 1 (SL1) is provided with a reduced performance. Available since January 2023, Galileo HAS is the first-ever global PPP service (Knight 2023). HAS SL1 comprises satellite orbit and clock corrections (i.e., non-dispersive effects), and dispersive effects, such as inter-frequency code biases, transmitted over Galileo E6-B signal and also through the internet (Fernandez-Hernandez et al. 2022). While the performance commitment for these products is still at the few-decimeter level (European GNSS Agency 2023), the current accuracy of the corrections is usually in the few-centimeter level, allowing a PPP accuracy (after convergence) already within specifications in most regions (Fernández-Hernandez et al. 2023). The positioning results presented in Naciri et al. (2023) are in line with these specifications, with average PPP horizontal and vertical errors of 13.1 cm and 17.6 cm, respectively, for the 95th percentile in kinematic mode.

In its full service, Service Level 2 (SL2), Galileo HAS will provide ionospheric delay corrections at least over Europe. In both SLs, users should be able to obtain a horizontal position error (HPE) of 20 cm (95%) and a vertical position error (VPE) of 40 cm (95%), after a convergence time below 5 min in SL1 and below 100 s in SL2 (European GNSS Agency 2021). The quality of the ionospheric corrections is, therefore, a key point for shortening the convergence time in SL2.

Since the early 2000s, the research group of Astronomy and GEomatics (gAGE) at the Universitat Politècnica of Catalunya (UPC) has been developing the concept of fast precise point positioning (F-PPP), see, for instance, Juan et al. (2012). The backbone of F-PPP is the precise modeling of the ionospheric delays, which enables users to achieve navigation solutions with centimeters errors after a few minutes of convergence time (as required for Galileo HAS). Unlike PPP–RTK, the scale of the ionospheric model can be continental or even global. More recently, gAGE/UPC, under a contract with the European Space Agency (ESA), is implementing the F-PPP concept in an end-to-end real-time tool, denominated as Ionospheric Corrections for HAS—IONO4HAS. The main characteristics of IONO4HAS were presented in Rovira-Garcia et al. (2021), and summarized in Table 1.

Notice that the F-PPP strategy, i.e., separating the parameter estimation into a geodetic filter and an ionospheric filter and using a grid representation for the ionospheric delays, handles only a few thousand parameters per filter, affordable to be implemented in a continental or even global service. In contrast, techniques like PPP–RTK, which interpolates slant ionospheric delays from the reference receivers to the user position, would require estimating and transmitting tens of thousands of parameters to offer an equivalent continental service. Indeed, to make possible the interpolation at any European location, it would be necessary to use hundreds of reference receivers

Table 1 F-PPP (IONO4HAS) central processing facility (CPF) general overview

Module	Parameters	Description
Geodetic filter	Input	Melbourne–Wübbena (MW) combination
		Ionospheric-free (IF) combination of pseudoranges and phases
		Predicted orbits
	Output	Unambiguous geometry-free combination of carrier phases
		Carrier phase ambiguities (constants) and phase biases
		Zenith tropospheric delay (random walk)
		Satellite and receiver clocks (white noise)
Ionospheric filter	Input	Unambiguous slant total electron content (STEC) values
		Irregular ionospheric grid points (IGP) distributed in two layers
	Output	Vertical total electron content (VTEC) at each IGP (random walk)
		Differential code biases (DCBs) for each satellite (random walk)

and to transmit thousands of ionospheric delays to make possible the interpolation at any European location.

The performance of the F-PPP ionospheric correction and its potential application to the Galileo HAS has been assessed previously. The test in the signal-in-space domain presented in Rovira-Garcia et al. (2021) demonstrated that the real-time corrections of the F-PPP ionospheric model outperformed standard ionospheric models, even when they are computed in post-process.

The test in the position domain proposed by Rovira-Garcia et al. (2020) indicates that using the position error as an indicator of the quality of the ionospheric corrections is not straightforward. Indeed, user navigation equations involve other parameters, apart from position correction, that shall be estimated in parallel (e.g., receiver clock, receiver hardware biases). This joint estimation introduces correlations in the covariance matrix, making it difficult to establish a direct relationship between the ionospheric prediction error and the error in the position. In Rovira-Garcia et al. (2020), a reduction in the number of estimation parameters was achieved by estimating the carrier phase ambiguities externally using the carrier code leveling (CCL) method (Mannucci et al. 1998), contributing to building navigation equations consisting of an almost direct relationship between the position error and the ionospheric prediction error.

The goal of the present work is to expose the performance assessment of the F-PPP model in the position domain, as in Rovira-Garcia et al. (2020), but in real-time mode and in a more accurate way based on the single-epoch (instantaneous) navigation using unambiguous wide-lane (WL) combination of carrier phases.

"Methodology" section describes the methodology used for relating the position error with the ionospheric prediction error. In "Data set" section, the data used for the ionospheric model testing and the ionospheric conditions during the testing period are presented. "Position domain results" section presents the results obtained during the testing period. Finally, "Conclusions" section summarizes the conclusions.

Methodology

The real-time data used as input by IONO4HAS comprise GPS and Galileo observations, from which it is possible to define a positioning test based on unambiguous WL combinations. The WL test improves the methodology presented in Rovira-Garcia et al. (2020), being the main novelty of the present work and described as follows:

For a receiver (rcv) and a satellite (sat), the WL combination ($L^{\text{sat}}_{\text{Wrcv}}$) is built using two different carrier phase observations at two different frequencies (L_i and L_j), by the following expression:

$$L^{\text{sat}}_{\text{Wrcv}} = \frac{f_i L^{\text{sat}}_{\text{ircv}} - f_j L^{\text{sat}}_{\text{jrcv}}}{f_i - f_j} \tag{1}$$

In GPS, the frequencies pair implemented are 1575,42 MHz and 1227,60 MHz (f_1 and f_2, respectively), whereas for the case of Galileo, the frequencies are f_1 and 1176,45 MHz (f_5). Equation (1) can be modeled as (Sanz et al. 2013):

$$\begin{aligned} L^{\text{sat}}_{\text{Wrcv}} =& \rho^{\text{sat}}_{\text{rcv}} + c\left(T_{\text{rcv}} - T^{\text{sat}}\right) + \text{Trop}^{\text{sat}}_{\text{rcv}} + \alpha_W \left(I^{\text{sat}}_{\text{rcv}} + \text{DCB}_{\text{rcv}} + \text{DCB}^{\text{sat}}\right) \\ &+ \lambda_W \left(N^{\text{sat}}_{\text{Wrcv}} + \delta_{\text{Wrcv}} + \delta^{\text{sat}}_{\text{W}}\right) + \varepsilon_{L_{\text{W}}} \end{aligned} \tag{2}$$

where $\rho^{\text{sat}}_{\text{rcv}}$ is the Euclidean distance between the sat and rcv antenna phase centers, c is the speed of light in the vacuum, T_{rcv} and T^{sat} are the receiver clock and satellite clock offsets with respect to GPS time, $\text{Trop}^{\text{sat}}_{\text{rcv}}$ is the tropospheric delay at the receiver position; $I^{\text{sat}}_{\text{rcv}} + \text{DCB}_{\text{rcv}} + \text{DCB}^{\text{sat}}$ are the terms for the ionospheric delay experienced by the signal, plus the receiver and satellite differential code biases (DCB), in total electron content units ($1\text{TECU} = 10^{16}\frac{e}{m^2}$), and $\alpha_W = \frac{40.3\times10^{16}}{f_i \cdot f_j}$ is a factor which converts the ionospheric delay from TECU to meters of L_{W}. The term $\left(N^{\text{sat}}_{\text{Wrcv}} + \delta_{\text{Wrcv}} + \delta^{\text{sat}}_{W}\right)$ is the carrier phase ambiguity that can be split into an integer part, $N^{\text{sat}}_{\text{Wrcv}}$, plus two real-valued phase biases δ_{rcv} and δ^{sat}. The wavelength of the L_{W} combination is denoted as $\lambda_{\text{W}} = \frac{c}{f_i - f_j}$. Finally, $\varepsilon_{L_{\text{W}}}$ stands for the carrier thermal noise, multipath, and all non-modeled effects.

Applying a first-order Taylor expansion around a given position of the receiver $r_{0_{\text{rcv}}}$, the geometric range can be written as $\rho^{\text{sat}}_{\text{rcv}} = \rho^{\text{sat}}_{0\text{rcv}} + G\Delta r$, where $\rho^{\text{sat}}_{0\text{rcv}}$ is the distance from the initial given position and the satellite, G is the geometry matrix and $\Delta r = r_{\text{rcv}} - r_{0_{\text{rcv}}}$. In this test, we will take $r_{0_{\text{rcv}}}$ as the precise coordinates of the receiver.

Following the PPP approach, the tropospheric delay can be split into two terms: A nominal value $\text{Trop}^{\text{sat}}_{0\text{rcv}}$ can be modeled as an ideal gas, plus the residual term $M^{\text{sat}}_{\text{rcv}} \cdot \text{ZTrop}_{\text{rcv}}$, where $M^{\text{sat}}_{\text{rcv}}$ is an obliquity factor depending on satellite elevation. $\text{ZTrop}_{\text{rcv}}$ is the zenith tropospheric delay, which is a parameter to be estimated together with the receiver coordinates and clock.

Satellite coordinates, clock offsets, and phase biases δ^{sat} are usual products of a real-time HAS provider. However, in this real-time implementation of F-PPP, we start from the predicted part of ultrarapid orbits produced by the Center for Orbit Determination in Europe (CODE)(Prange et al. 2016), which have errors of just some centimeters (Chen et al. 2021), but similar products from any real-time service could be used as well.

The geodetic filter in the F-PPP CPF accurately estimates satellite clocks and phase biases. Additionally, the CPF can calculate carrier integer ambiguities, receiver clock offset, and zenith tropospheric delay to use a rover receiver in the testing.

Thence, it is possible to use the observed $L^{\text{sat}}_{\text{Wrcv}}$ and all the previously defined terms, which are accurately modeled, to define the following residuals:

$$\Delta L^{\text{sat}}_{\text{Wrcv}} = L^{\text{sat}}_{\text{Wrcv}} - \rho^{\text{sat}}_{0\text{rcv}} + cT^{\text{sat}} - \text{Trop}^{\text{sat}}_{0\text{rcv}} - \lambda_W\left(N^{\text{sat}}_{\text{Wrcv}} + \delta^{\text{sat}}_{\text{W}}\right) \tag{3}$$

where all the parameters can be precisely known by processing ionosphere-free (IF) combinations of measurements (Sanz et al. 2013).

From (2) and (3), we can rewrite the measurement equation as follows, where the receiver clock term T_{rcv} includes now the DCB_{rcv} and phase biases δ_{Wrcv}:

$$\Delta L^{\text{sat}}_{\text{Wrcv}} - \alpha_W\left(I^{\text{sat}}_{\text{rcv}} + \text{DCB}^{\text{sat}}\right) = G\Delta r + cT_{\text{rcv}} + M^{\text{sat}}_{\text{rcv}}\text{ZTrop}_{\text{rcv}} + \varepsilon_{L_W} \tag{4}$$

where the ionospheric delay $I^{\text{sat}}_{\text{rcv}}$ and satellite DCB^{sat} are the corrections to test, and the error in Δr estimation is an indicator of the goodness of such corrections. Given that the receiver clock offset and the zenith tropospheric delay for the rover receivers are also estimated, they can be fixed and placed on the left side of (4).

Equation (4) represents a pseudorange modeling that can be solved in a single epoch, treating all parameters (receiver coordinates, clock and troposphere) as white noise parameters. Indeed, equation (4) establishes a direct relationship between rover position error and ionospheric prediction accuracy. This link can be strengthened using external estimates of the tropospheric term $\text{ZTrop}_{\text{rcv}}$ and receiver clock T_{rcv}, such as the estimates calculated by the CPF. In this way, as all the parameters are estimated using a white noise process, errors in the ionospheric prediction directly impact the position error estimate. In this instantaneous positioning method, data from previous epochs do not participate, emulating a continuous cold start.

Data set

The GNSS observations from permanent stations are collected in real time using the Networked Transport of RTCM via Internet Protocol (NTRIP). The IONO4HAS processes input data files at a rate of five seconds, sufficient to build a robust cycle slip detector. Once these higher rate observations are exploited, the IONO4HAS tool decimates the data at a lower rate of 30 s, which is ample for computing the subsequent program steps. We have selected a dataset of 281 days in 2022, from day-of-the-year (DoY) 40 to DoY 320, when a stable version of the IONO4HAS tool was already running.

Receivers distribution

The IONO4HAS tool operates on a daily and automatic basis since the beginning of 2022, collecting GNSS data streams from approximately 200 permanent stations belonging to the networks IGS, EUREF, and AUSCORS (Fig. 1). For this work, the designed network focuses on Europe, with a total of 80 receivers, all of them collecting GPS data and 30 collecting both GPS and Galileo data. For testing the IONO4HAS corrections, 15 European receivers have been used as users of the service (rovers).

From the network of Fig. 1, three different regions (or subnetworks) are defined in Europe to test the ionospheric

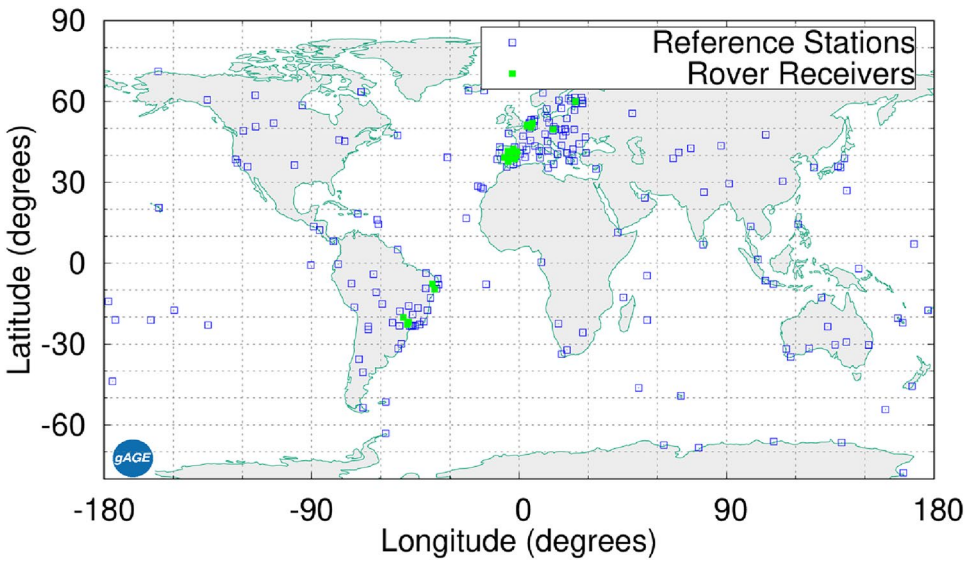

Fig. 1 IONO4HAS network of GNSS receivers. The reference stations used to compute the ionosphere corrections are depicted in blue squares, while the receivers used for testing the ionospheric corrections are depicted as green squares

corrections and satellite DCBs computed using the F-PPP CPF. A mid-latitude network located in the Iberian Peninsula (top panel of Fig. 2), between 35 and 43 °N. It comprises nine rover receivers surrounded by eleven global reference stations. Rovers are located at distances ranging from 100 to over 300 km from the nearest reference stations (see Table 2). It is important to note that being the Sun the main driver of the ionospheric activity, in a real-time context a rover benefits from ionospheric delays experienced by a permanent station only if it is positioned to the east (i.e., before affecting the rover itself), under similar local time conditions. Consequently, the reference station to consider should be the closest station from the east (effective distance). This is the main drawback of real-time ionospheric models compared to post-processed models, where all measurements (future and past, corresponding to east and west) can be involved in the computation at any epoch.

A mid-high-latitude network, between 50 and 55 °N, involving GNSS receivers located in Belgium and the Netherlands. The middle panel of Fig. 2 depicts the four rover receivers and nine reference stations surrounding the rovers. Lastly, a high-latitude network, between 59 and 62 °N, located in the Gulf of Finland, with two rover receivers and seven reference stations within Finland and Estonia, as seen in the bottom panel of Fig. 2. Table 2 summarizes the main features within the three networks.

Ionospheric activity during the data window

The ionospheric activity during these days was analyzed using the Along Arc TEC Ratio (AATR) index for different GNSS stations located at representative latitudes in the subnetworks. The AATR is a reliable index for ionospheric studies that can be computed from actual GNSS carrier phase measurements at a low sampling rate (Juan et al. 2018). Juan et al. (2018) and Belehaki et al. (2020) defined the level of ionospheric activity using the AATR as low-quiet (up to 0.5 TECU/min), medium-moderate (up to 1 TECU/min), and high-large (greater than 1 TECU/min). These levels are depicted in Fig. 3 using a green line to threshold the low and medium ionospheric activity regions, and using a red line to threshold the medium and high ionospheric activity regions.

As seen in Fig. 3, the ionospheric activity was not significantly high. In particular, the rover MET3 experienced some specific days with high ionospheric activity (related to space weather events), whereas rover KOS1 was under low ionospheric activity during the entire testing period. The Iberian Peninsula rovers, RIO1 and SONS, had moderate ionospheric activity related to equinoxes or with the 27-day period of the solar synodic rotation.

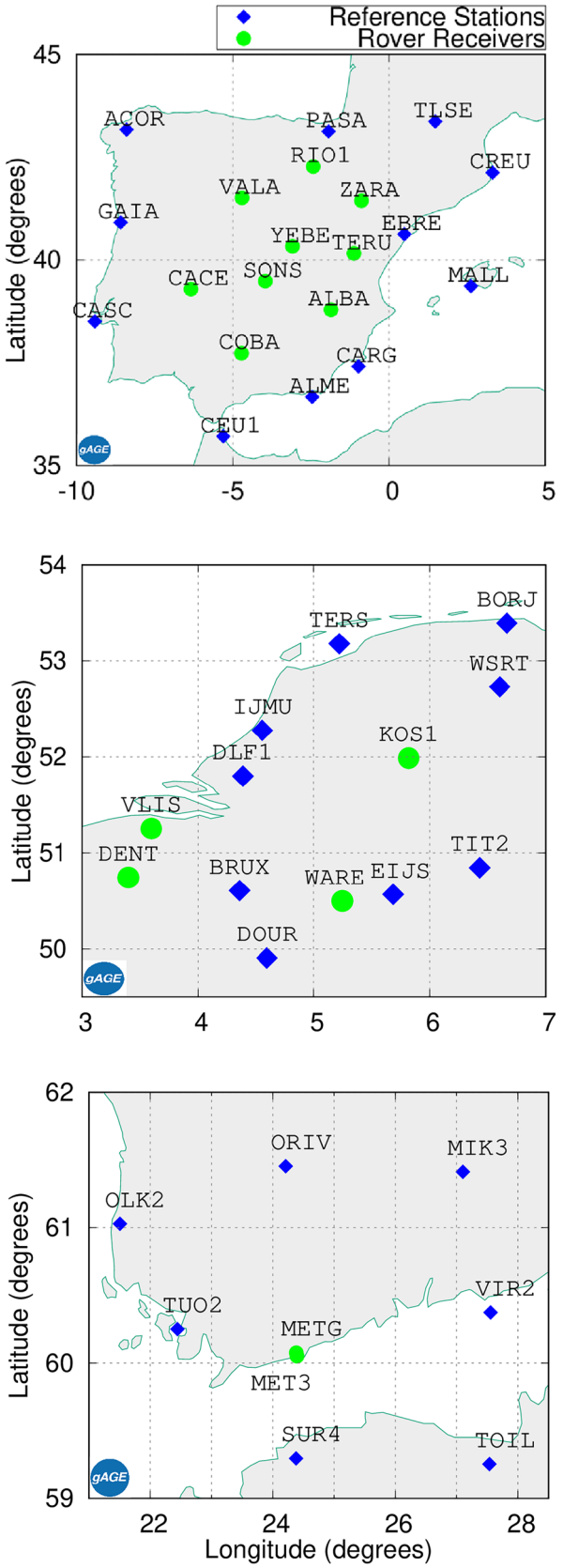

Fig. 2 Designed subnetworks: Iberian (top), Belgium (middle), and Finnish (bottom) networks. Reference stations are depicted in blue diamonds. Rovers are indicated using green circles

Table 2 Baselines of the subnetworks

Network	Rover receiver	Longitude (°)	Latitude (°)	Nearest permanent station	Distance (km)	Data type
Iberian Peninsula	RIO1	−2.42	42.27	PASA	103.5	GPS
	ZARA	−0.88	41.44	EBRE	146.4	GPS, GAL
	TERU	−1.12	40.16	EBRE	146.5	GPS
	ALBA	−1.85	38.78	CARG	171.6	GPS
	COBA	−4.72	37.72	ALME	232.5	GPS
	CACE	−6.34	39.29	CEU1	408.4	GPS, GAL
	VALA	−4.70	41.51	PASA	290.6	GPS
	SONS	−3.96	39.48	ALME	339.8	GPS
	YEBE	−3.08	40.33	EBRE	304.6	GPS
Belgium	WARE	5.24	50.50	EIJS	31.89	GPS
	DENT	3.39	50.74	BRUX	69.22	GPS
	VLIS	3.59	51.25	DLF1	81.50	GPS
	KOS1	5.81	51.98	WRST	98.3	GPS
Finnish	MET3	24.4	60.1	SUR4	84.1	GPS, GAL
	METG	24.4	60.1	SUR4	86.8	GPS, GAL

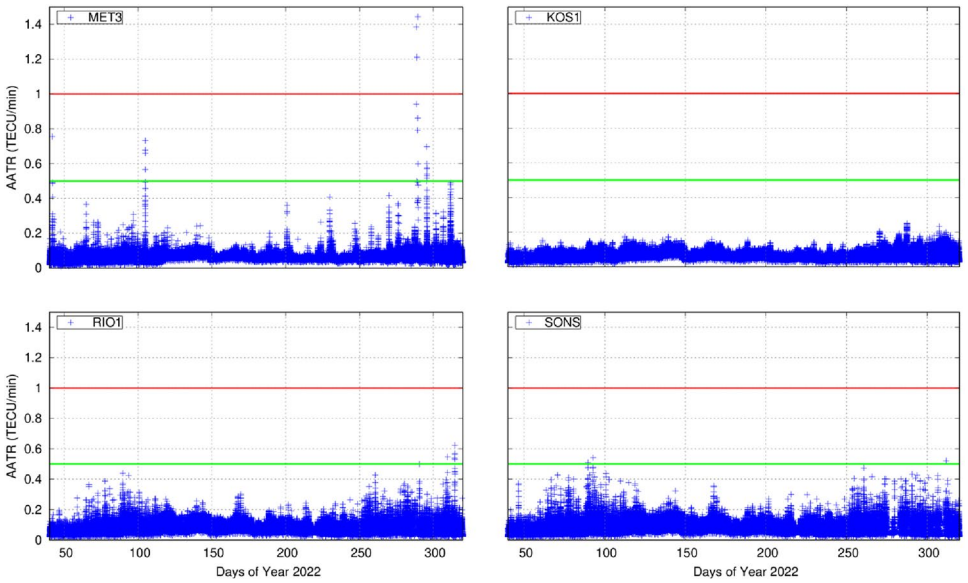

Fig. 3 Ionospheric activity assessed by the AATR index during the study campaign. The top left plot corresponds to MET3 receiver in the Finnish network. The top right plot represents KOS1 receiver in the Belgium network. Finally, the Iberian network is presented in the bottom plots: RIO1 and SONS on the left- and right-side plots, respectively. Horizontal lines indicate ionospheric activity: green for moderate activity and red for high activity

Position domain results

The main benefit of high-accuracy ionosphere corrections is the capability to obtain positioning with errors at the level of decimeters with a short convergence time. With this goal in mind, this section assesses the positioning performance over the full data campaign. These single-epoch positioning results are computed by applying the unambiguous WL combination explained in "Methodology"section.

Statistical characterization

From Figs. 4, 5 and 6, it is displayed performance examples for selected stations in each network, featuring different baselines and latitudes relative to the nearest reference station. The statistical representation of the error distribution is characterized using the complementary cumulative distribution function (CCDF, also denoted as 1-CDF) over four representative receivers. The CCDF tool allows us to determine the probability (*Y*-axis) of each data point on the

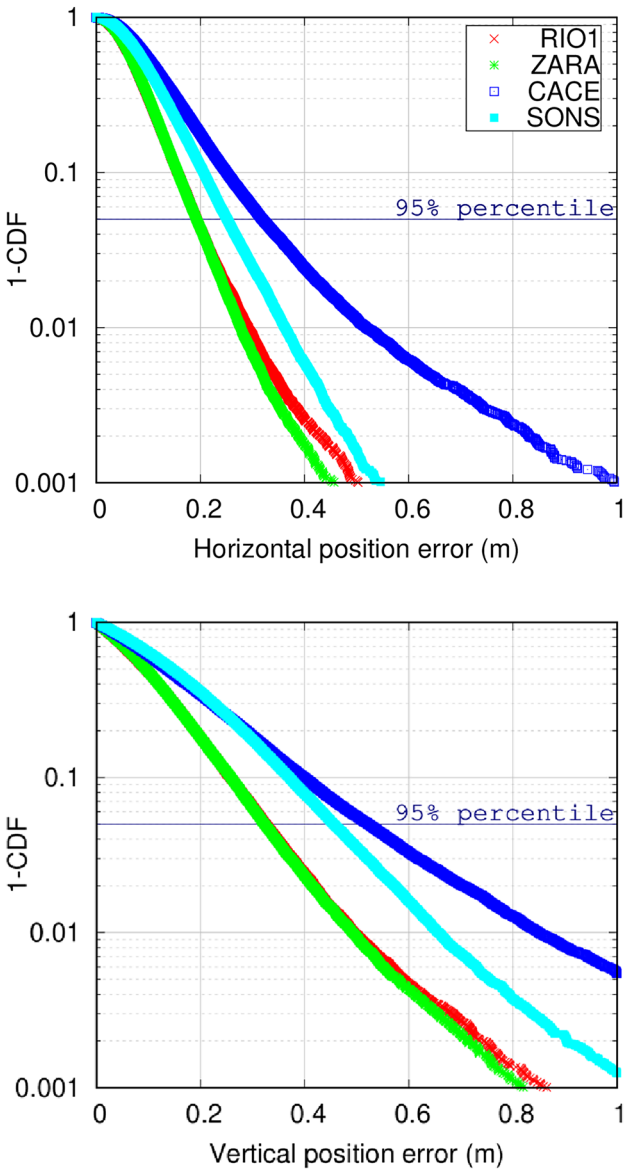

Fig. 4 Distribution of positioning errors in the Iberian network. 1-CDF for the HPE (top) and VPE (bottom)

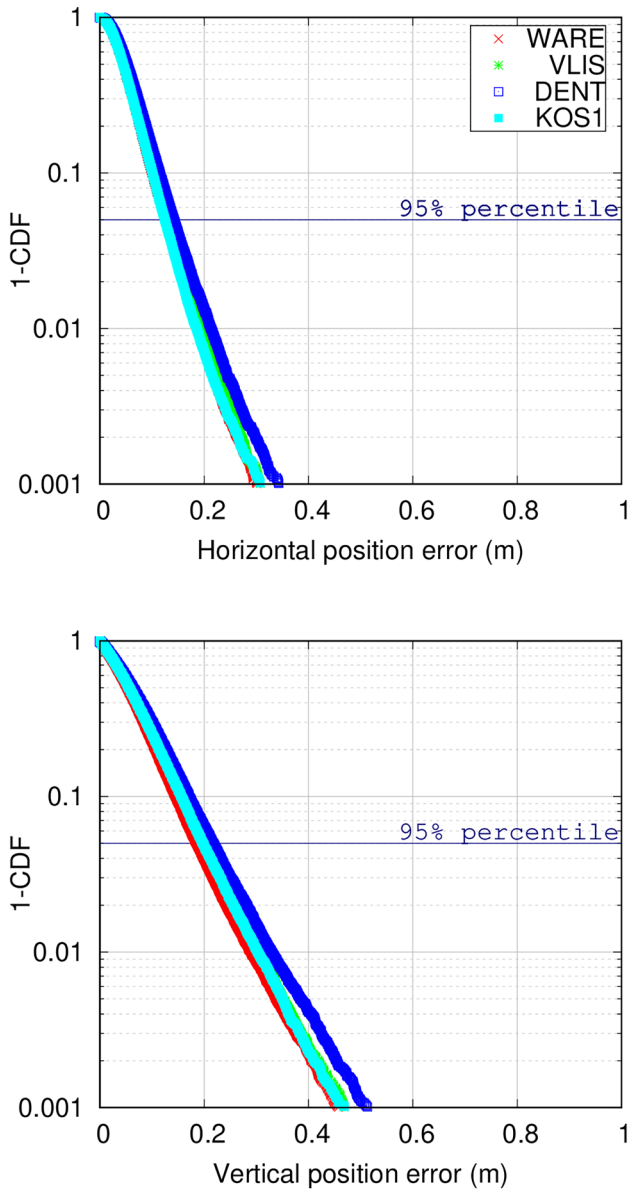

Fig. 5 Distribution of positioning errors in the Belgium network. 1-CDF positioning for the HPE (top) and VPE (bottom)

graph (predictions) of having an error larger than the value on the *X*-axis.

Starting with the Iberian Peninsula (Fig. 4), it is observed that 95th percentile ranges from 20 to 30 cm and from 20 to 50 cm, for the HPE and VPE components, respectively. Similar results were obtained assessing the Belgium network (Fig. 5). In this case, baselines are shorter, with WARE and KOS1 stations being located about 32 km and 98 km from the nearest eastern reference station, respectively. Figure 6 shows the 1-CDF for the stations MET3 and METG in the finnish network case. Notice that, although the baselines to the nearest reference receiver are similar to those in the mid-high-latitude network, the positioning errors are higher for these two northern receivers. This is related to the higher ionospheric activity affecting this region, as seen in Fig. 3. On the other hand, it is worth noticing that the baseline between MET3 and METG is only around 3 km, so one should expect similar quality of the ionospheric corrections and similar results in the positioning test. The slight differences between both solutions can be related to the fact that MET3 and METG are equipped with different receiver types (Javad and Septentrio, respectively), having different measurement noises.

Table 3 presents the 95th percentile of HPE and VPE for all the rovers within each sub-network. In the case of the Iberian network, despite a noticeable degradation

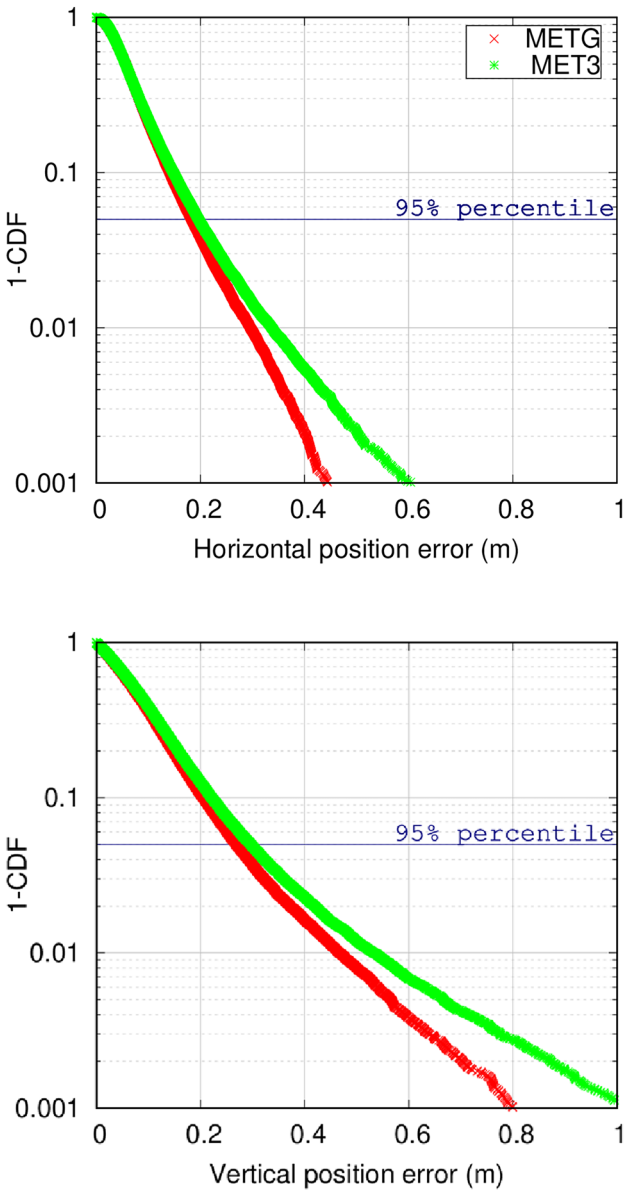

Fig. 6 Distribution of positioning errors in the Finnish network. 1-CDF for the HPE (top) and VPE (bottom)

linked to the baseline distance, the case with the greatest baseline distance (408 km, corresponding to CACE from CEU1) reports values around 30 cm in HPE and 50 cm in VPE. Regarding the Belgium network, it must be noted that although the baseline of station KOS1 is about three times longer than the baseline of WARE, the 95th percentile of positioning error is similar for both HPE and VPE components: about 15 cm and 20 cm, respectively. Finally, in the Finnish network case, the 95th percentile of the positioning error for both receivers reaches up to 20 and 30 cm in the HPE and VPE components, respectively, which fulfill the Galileo HAS requirements (which will be discussed in the next sections) and are well covered by the confident levels of the ionospheric corrections.

Overall, for these different European latitudes, the contribution of the ionospheric mismodeling to the implementation of the single-epoch positioning technique results in a positioning error below 0.3 m and 0.5 m for the horizontal and vertical components, respectively. These results are in line with the expected output of (4), in which constraining the tropospheric and receiver clock terms produces a minor worsening of the achieved positioning.

It is worth mentioning that once the instantaneous positioning has been achieved (i.e., the carrier phase ambiguity of the WL combination is known), the capability of fixing the ambiguity on L1 or E1 is available, which would allow building the unambiguous ionosphere-free combination, navigating with a precision of few centimeters in the horizontal component and being free from ionospheric effects.

Validation of the F-PPP results

To illustrate the benefits of employing F-PPP corrections, Table 3 compares the instantaneous positioning for the complete set of rovers receivers at the 95th percentile, comparing three different cases: (1) when the F-PPP ionospheric corrections are implemented, (2) when employing a standard ionospheric model such as the IGS rapid product (IGRG), computed in post-processing, and (3) when the solution is obtained without the utilization of any ionospheric model, i.e., the standard PPP solution (referred in Table 3 as "NO IONO").

It is evident that navigation without implementing ionospheric model does not offer any advantage in resolving the wide-lane ambiguity. The navigation solution relies on pseudorange measurements, specifically on the ionospheric-free combination of pseudorange. As anticipated, this results in a positioning error of around 1 m in the instantaneous positioning. However, when an ionospheric model is employed, the unambiguous wide-lane combination can be corrected from its ionospheric delay and the error in instantaneous positioning is driven by the quality of the chosen ionospheric model. In this context, it can be concluded that the F-PPP ionospheric model surpasses the IGRG model, corroborating the findings in Rovira-Garcia et al. (2021).

Confidence level of the ionospheric corrections

It is possible to evaluate the confidence of the F-PPP corrections through the actual position error. This is done by comparing the predicted error value (i.e., the standard deviation extracted from the diagonal of the covariance matrix of estimates (Rovira-Garcia et al. 2015)) and the resulting actual positioning error. This evaluation concept is similar to the one implemented in civil aviation to test the satellite-based

Table 3 Ionospheric corrections assessment through instantaneous positioning error (95th percentile)

Network	Station	95th percentile of horizontal error (m)			95th percentile of vertical error (m)		
		F-PPP	IGRG	NO IONO	F-PPP	IGRG	NO IONO
Iberian Peninsula	RIO1	0.19	0.58	2.05	0.32	0.91	3.06
	TERU	0.21	0.61	1.70	0.41	1.07	2.59
	ZARA	0.19	0.60	1.83	0.32	1.00	3.04
	ALBA	0.23	0.56	2.20	0.37	0.95	3.46
	COBA	0.25	0.61	1.65	0.41	1.06	2.72
	VALA	0.22	0.57	1.53	0.37	0.90	2.33
	YEBE	0.22	0.65	2.06	0.46	1.15	3.29
	SONS	0.25	0.62	1.77	0.45	1.10	2.95
	CACE	0.32	0.71	2.32	0.52	1.22	3.98
Belgium	WARE	0.12	0.56	1.25	0.18	0.92	1.94
	VLIS	0.13	0.54	1.61	0.20	0.85	2.50
	DENT	0.14	0.57	1.23	0.21	0.94	1.97
	KOS1	0.12	0.59	1.23	0.19	1.00	2.07
Finnish	METG	0.18	0.37	0.86	0.26	0.59	1.30
	MET3	0.19	0.61	1.59	0.29	1.08	2.70

augmentation system (SBAS) integrity using the so-called Stanford diagrams (Walter et al. 1999) (Tossaint et al. 2007), where the predicted error is inflated by a factor 6.0, for the horizontal component, or 5.33, for the vertical component. These values correspond to k-factors of a Gaussian distribution with a probability of 2×10^{-9} and 1×10^{-7}, respectively. In SBAS, these inflation factors lead to protection levels that secure users against unreliable corrections. Although IONO-4HAS does not target the same integrity level of civil aviation, our implementation is based on the same basic SBAS principle to check the confidence of the predicted errors.

Figure 7 depicts this confidence test applied to all the rovers within the Iberian, Belgium, and Finnish networks. In this way, the results can be considered satisfactory when there is a consistently higher number of epochs (points) in which the actual positioning error is lower than the confidence bound (inflated predicted error). Graphically, this is observed as the epochs laying above the 45° line (where the expected value is equal to the real value, i.e., $x=y$).

The test provides a robust perspective of the confidence of the IONO4HAS tool corrections, being 100% of the position (1.26×10^6 epochs) clearly above the bisector. The majority of the points located closer to the bisector correspond to days within the Finnish network experiencing high ionospheric activity in the region (specifically, DoY 312 in Fig. 3), indicating that, for this region, the ionospheric activity should be taken into account in the F-PPP tool. During these specific periods, the predicted errors of the ionospheric corrections should be enlarged, for instance, by increasing the process noises of the ionospheric model taking into account the AATR.

Conclusively, an additional objective of the proposed test is to provide a methodology for characterizing formal errors associated with ionospheric correction values. This predicted error is a valuable information parameter, allowing any user of the service to appropriately weigh their measurements within the navigation filter. Typically, both horizontal and vertical formal errors are observed at the level of the decimeter (1 sigma).

Conclusions

The present work examined the results obtained during 281 days of running the F-PPP ionospheric model in an end-to-end real-time mode, obtained from a set of rover receivers located at different latitudes in Europe with distances to the closer reference receivers ranging from tens to 400 km.

The resulting assessment has implemented a novel instantaneous positioning test based on the unambiguous WL combination. The test results show a clear connection between the error in rover position estimation and the accuracy of ionospheric corrections, with instantaneous positioning errors between one and three decimeters for the horizontal component and two and five decimeters for the vertical component, both at the 95th percentile. These results confirm that the IONO4HAS tool can be an adequate candidate for providing a HAS over Europe. Finally, it has been shown that the F-PPP ionospheric model can provide accurate enough ionospheric corrections and confident values of their predicted errors.

One of the main goals of the F-PPP ionospheric model is to provide global coverage. The current status of the

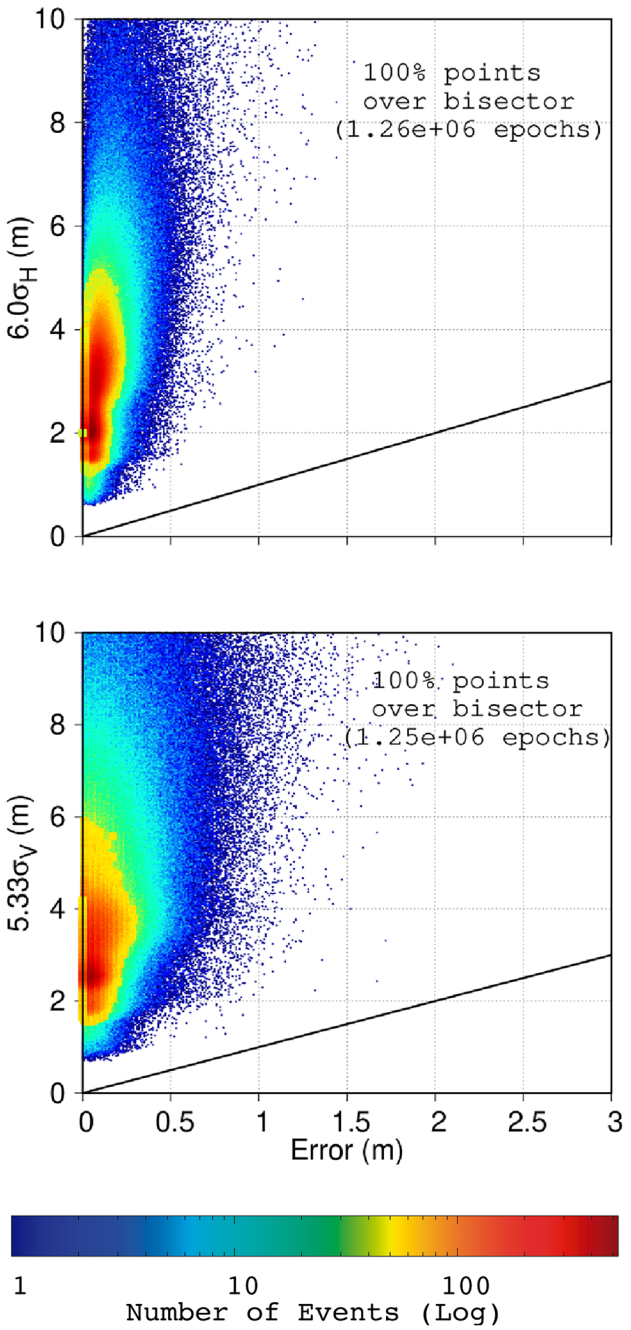

Fig. 7 Confidence level of the ionospheric corrections versus actual HPE (top) and VPE (bottom) for all the rover receivers

developed tool and implemented techniques enables us to consider in a near future expanding this study beyond Europe to complex regions, such as Brazil, where ionospheric activity presents more challenging characteristics to model. Moreover, it is also feasible to evaluate user positioning by implementing different strategies, including the kinematic mode instead of the instantaneous positioning presented in this work.

Acknowledgements The authors would like to thank the International GNSS Service for the availability of precise products and GNSS data, as well as the GNSS observations open data service provided by The EUREF Permanent Network (EPN) and the Geoscience Australia AUSCORS NTRIP Broadcaster.

Author contributions JMJ and CCT proposed the general idea of this contribution and initiated the work. JMJ and CCT designed and developed the IONO4HAS real-time tool used in the study. CCT, JS, and JMJ analyzed the results and wrote the manuscript. ARG, DB, GGC, IFH, and ROP contributed to the technical discussion and organization of the manuscript. All authors provided advice and critically reviewed the manuscript.

Funding Open Access funding provided thanks to the CRUE-CSIC agreement with Springer Nature. The present work was supported by the ESA contracts 4000128823/19/NL/AS (CCN1) and 4000128823/19/NL/AS (CCN2), and by the Spanish Ministry of Science and Innovation and the European Community FEDER through the project PID2022-138485OB-I00.

Data availability Precise products (orbits, satellite clocks, and troposphere) can be found in the International GNSS Service server https://cddis.nasa.gov/archive/gnss/products. GNSS observations can be downloaded from https://cddis.nasa.gov/archive/gnss/data/highrate/. The real-time results and products of the IONO4HAS tool presented in this publication can be accessed through the web server: https://server.gage.upc.edu/iono4has/

Declarations

Competing interests The authors declare no competing interests.

Conflict of interest The content of this article does not necessarily reflect the official position of the authors' organizations. Responsibility for the information and views set out in this article lies entirely with the authors.

Ethical approval This declaration is not relevant to the content of the present: "not applicable."

Open Access This article is licensed under a Creative Commons Attribution 4.0 International License, which permits use, sharing, adaptation, distribution and reproduction in any medium or format, as long as you give appropriate credit to the original author(s) and the source, provide a link to the Creative Commons licence, and indicate if changes were made. The images or other third party material in this article are included in the article's Creative Commons licence, unless indicated otherwise in a credit line to the material. If material is not included in the article's Creative Commons licence and your intended use is not permitted by statutory regulation or exceeds the permitted use, you will need to obtain permission directly from the copyright holder. To view a copy of this licence, visit http://creativecommons.org/licenses/by/4.0/.

References

Belehaki A et al (2020) An overview of methodologies for real-time detection, characterisation and tracking of traveling ionospheric disturbances developed in the TechTIDE project. J Space Weather Space Clim 10:42. https://doi.org/10.1051/swsc/2020043

Chen Q, Song S, Zhou W (2021) Accuracy analysis of GNSS hourly ultra-rapid orbit and clock products from SHAO AC of iGMAS. Remote Sens 13(5):1022

Duong V, Harima K, Choy S, Laurichesse D, Rizos C (2020) Assessing the performance of multi-frequency GPS, Galileo and BeiDou PPP ambiguity resolution. J Spat Sci 65(1):61–78. https://doi.org/10.1080/14498596.2019.1658652

European GNSS Agency (2021) Galileo high accuracy service (HAS): info note. Publications Office. https://doi.org/10.2878/581340

European GNSS Agency (2023) Galileo high accuracy service : service definition document (HAS SDD) : issue 1.0, January 2023. Publications Office of the European Union. https://doi.org/10.2878/265974

Fernandez-Hernandez I et al (2022) Galileo high accuracy service: initial definition and performance. GPS Solut 26(3):65. https://doi.org/10.1007/s10291-022-01247-x

Fernández-Hernandez I et al (2023) Galileo authentication and high accuracy: getting to the truth. Inside GNSS Magazine, Eugene, pp 58–65

Hadas T, Bosy J (2015) IGS RTS precise orbits and clocks verification and quality degradation over time. GPS Solut 19:93–105

Juan JM et al (2012) Enhanced precise point positioning for GNSS users. IEEE Trans Geosci Remote Sens 50(10):4213–4222

Juan JM, Sanz J, Rovira-Garcia A, González-Casado G, Ibáñez D, Perez RO (2018) AATR an ionospheric activity indicator specifically based on GNSS measurements. J Space Weather Space Clim 8:A14

Knight R (2023) Galileo high accuracy service now operational, providing corrections worldwide for free. INSIDE GNSS Magazine, Eugene

Laurichesse D, Banville S (2018) Innovation: instantaneous centimeter-level multi-frequency precise point positioning. GPS World, Innovation column 4 July.

Mannucci AJ, Wilson BD, Yuan DN, Ho CH, Lindqwister UJ, Runge TF (1998) A global mapping technique for GPS-derived ionospheric total electron content measurements. Radio Sci 33(3):565–582

Naciri N, Bisnath S (2023) RTK-quality positioning with global precise point positioning corrections. Navigation J Inst Nav 70(3):navi.575. https://doi.org/10.33012/navi.575

Naciri N, Yi D, Bisnath S, Javier de Blas F, Capua R (2023) Assessment of Galileo high accuracy service (HAS) test signals and preliminary positioning performance. GPS Solut 27:73. https://doi.org/10.1007/s10291-023-01410-y

Prange L, Dach R, Lutz S, Schaer S, Jäggi A (2016) The CODE MGEX orbit and clock solution. In: Rizos C, Willis P (eds) IAG 150 Years. Springer International Publishing, Cham, pp 767–773

Psychas D, Verhagen S, Liu X, Memarzadeh Y, Visser H (2018) Assessment of ionospheric corrections for PPP–RTK using regional ionosphere modeling. Meas Sci Technol 30(1):14001

Rovira-Garcia A, Juan JM, Sanz J, Gonzalez-Casado G (2015) A worldwide ionospheric model for fast precise point positioning. IEEE Trans Geosci Remote Sens 53(8):4596–4604

Rovira-Garcia A, Ibáñez-Segura D, Orús-Perez R, Juan JM, Sanz J, González-Casado G (2020) Assessing the quality of ionospheric models through GNSS positioning error: methodology and results. GPS Solut 24(1):4

Rovira-Garcia A, Timoté CC, Juan JM, Sanz J, González-Casado G, Fernández-Hernández I, Orus-Perez R, Blonski D (2021) Ionospheric corrections tailored to the Galileo high accuracy service. J Geodesy 95(12):130

Sanz-Subirana J, Juan-Zornoza JM, Hernández-Pajares M (2013) GNSS data processing, Vol. I: fundamentals and algorithms. ESA Communications. https://server.gage.upc.edu/TEACHING_MATERIAL/GNSS_Book/ESA_GNSS-Book_TM-23_Vol_I.pdf

Tossaint M, Samson J, Toran F, Ventura-Traveset J, Hernández-Pajares M, Juan JM, Sanz J, Ramos-Bosch P (2007) The Stanford–ESA integrity diagram: a new tool for the user domain SBAS integrity assessment. Navigation 54(2):153–162

Walter T, Hansen A, Enge P (1999) Validation of the WAAS MOPS integrity equation. In: Proceedings of the 55th annual meeting of the institute of navigation (1999), pp 217–226

Wübbena G, Schmitz M, Bagge A (2005) PPP–RTK: precise point positioning using state-space representation in RTK networks. In: Proceedings of the 18th international technical meeting of the satellite division of the institute of navigation (ION GNSS 2005), pp 2584–2594

Zumberge JF, Heflin MB, Jefferson DC, Watkins MM, Webb FH (1997) Precise point positioning for the efficient and robust analysis of GPS data from large networks. J Geophys Res Solid Earth 102(B3):5005–5017. https://doi.org/10.1029/96jb03860

Publisher's Note Springer Nature remains neutral with regard to jurisdictional claims in published maps and institutional affiliations.



C. C. Timote holds a Master's degree in GNSS from the French Civil Aviation University (ENAC) and a PhD in Aerospace Science and Technology from the Technical University of Catalonia (UPC). He is a postdoctoral researcher at gAGE, working on ionospheric monitoring and modeling using GNSS signals.



J. M. Juan is a Tenure Full Professor at the Department of Physics (UPC) and a member of gAGE since 1988. He has published over 70 papers in peer-reviewed journals and more than 200 works in Meeting proceedings related to GNSS, with four best paper awards from the US Institute of Navigation. He is a co-author of five patents on GNSS and four books on GNSS Data Processing.



J. Sanz is a Tenure Full Professor at the Department of Mathematics (UPC) and a member of gAGE since 1988. He has published over 70 papers in peer-reviewed journals and more than 200 works in meeting proceedings related to GNSS, with four best paper awards from the US Institute of Navigation. He is a co-author of five patents on GNSS and four books on GNSS Data Processing.



A. Rovira-Garcia is a Serra Hunter Fellow with the Department of Physics (UPC) and a member of gAGE since 2009. He co-authors 29 papers in peer-reviewed journals, two book chapters, and over 50 works in meeting proceedings, with one best presentation award from the US Institute of Navigation. His research interests are focused on high-accuracy navigation under scintillation.



G. González-Casado is with the Department of Mathematics (UPC) and a member of gAGE since 2009. His research interests are focused on ionospheric modeling based on GNSS and radio occultations, ground and satellite-based augmentation systems, and the study and development of GNSS applications for the study of the ionosphere and plasmasphere.



R. Orús-Pérez has a Physics degree from the University of Barcelona (UB) and a PhD in Aerospace Science and Technology from the Technical University of Catalonia (UPC). Since 2010 he has been working in the RF Payloads and Technology Division of ESA/ESTEC as a Propagation Engineer on activities related to radio-wave propagation in the troposphere and ionosphere for GNSS and other ESA missions.

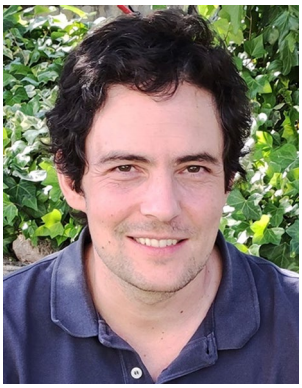

I. Fernández-Hernández has an MSc from ICAI and a PhD from Aalborg University, both in electronics engineering. He works for the European Commission DG DEFIS, in charge of Galileo authentication and high accuracy. He is also a visiting professor at KU Leuven.



D. Blonski is a Navigation System Performance Engineer at the European Space Research and Technology Centre of the European Space Agency in Noordwijk, NL, where he is contributing to the development of the European Navigation Systems as a member of the ESA Directorate of Navigation.